Genes & Diseases (2024) 11, 101141

Available online at www.sciencedirect.com

ScienceDirect

journal homepage: www.keaipublishing.com/en/journals/genes-diseases

RAPID COMMUNICATION

A prognostic model of patients with pancreatic cancer based on four N^6-methyladenosine-related lncRNAs and analysis of related immune infiltration

Pancreatic cancer is one of the most lethal malignant tumors in the world. Despite advances in diagnosis and treatment, the five-year survival rate for pancreatic cancer patients remains only 9%.[1] Pancreatic adenocarcinoma (PAAD) belongs to pancreatic cancer, which occupies 85% of the whole pancreatic cancer.[2] Reversible modification of N^6-methyladenosine (m^{6}A) has been shown to be involved in cancer progression, resulting in up-regulation of oncogene expression or down-regulation of tumor-suppressing genes and may affect the prognosis of patients with pancreatic cancer.[3] In pancreatic cancer, increasing evidence suggests that aberrant expression of lncRNA is related to tumor cell proliferation and metastasis.[4,5] Although m^{6}A can regulate lncRNA formation, the role of m^{6}A-related lncRNAs in PAAD remains unclear.

In this study, we aim to explore the prognostic value and the role of m^{6}A-related lncRNAs in the immune response of patients with PAAD. We established a novel m^{6}A prognostic model to predict overall survival in PAAD patients. Besides, we focused on the relationship between m^{6}A-related lncRNA and tumor immune microenvironment. M^{6}A RNA methylation regulator plays a key role in the progression of malignant tumors. Based on the RNA-seq data and corresponding clinical information of cancer samples and paracancer tissue samples from PAAD patients from the TCGA database, 23 m^{6}A regulating genes were extracted. In order to identify potential m^{6}A-related lncRNAs, we used the Pearson correlation coefficient to evaluate the relationship between m^{6}A methylation regulators and lncRNAs. The results showed that 87 interactions and 56 m^{6}A-related lncRNAs were identified (absolute correlation coefficient $>$ 0.6, $P < 0.05$) (Fig. S1A). Combined with PAAD survival information of TCGA, we screened out m^{6}A-related prognostic lncRNAs from 56 m^{6}A-related lncRNAs by univariate Cox regression analysis ($P < 0.05$). Further, LASSO regression analysis found that 11 m^{6}A-associated lncRNAs were significantly associated with overall survival in PAAD patients (Fig. S1B and Table S2). We used heatmap analysis to compare the expression of m^{6}A-associated lncRNAs in tumor and normal tissues associated with patient survival (Fig. S1C). Compared with normal tissue samples, the expression levels of the 11 m^{6}A-related lncRNAs in tumor tissue samples were significantly decreased (Fig. S1D). Figure S1E showed the correlation between m^{6}A-related prognostic lncRNAs.

To comprehensively explain the biological characteristics of the m^{6}A-related prognostic lncRNAs, the ConsensusClusterPlus package was used to divide the 177 PAAD patients into two clusters with higher stability (Fig. S2A–D). Then, we determined whether there were significant differences in clinicopathologic features and immune checkpoint PD-L1 (CD274) expression between the two clusters by using the heatmap package and limma package. The heatmap shows significant differences between the two subgroups, mainly in stage and tumor size (Fig. S3A). We found a significant difference in PD-L1 expression between the two clusters but no significant difference between tumor and normal tissues (Fig. S2A–D). Patients in cluster 1 had worse survival probability than patients in cluster 2 ($P < 0.001$) (Fig. S3D). These results suggest that cluster subtypes identified by the expression of m^{6}A-related prognostic lncRNAs were closely associated with patient prognosis and PD-L1 expression.

To further explore the role of m^{6}A-related prognostic lncRNAs in the biological processes and signaling pathways of PAAD, we conducted KEGG gene enrichment analysis for m^{6}A-related prognostic lncRNAs. Then, we used GSEA to

Peer review under responsibility of Chongqing Medical University.

https://doi.org/10.1016/j.gendis.2023.101141

perform functional enrichment analysis on the expression of m^{6}A-related prognostic lncRNAs in the two clusters to gain insight into the involvement in the biological processes and signaling pathways underlying PAAD. We integrated the expression data of m^{6}A-related prognostic lncRNAs with the KEGG database, calculated the enrichment scores of gene sets, and evaluated the statistical significance, thereby elucidating the potential distinct regulatory mechanisms between the two clusters. Our enrichment analysis results showed that the m^{6}A-related prognostic lncRNAs in cluster 2 were significantly enriched in the chemokine signaling pathway, cytokine—cytokine receptor interaction, MAPK signaling pathway, neuroactive ligand—receptor interaction, regulation of actin cytoskeleton, calcium signaling pathway, and focal adhesion. Conversely, m^{6}A-related prognostic lncRNAs in cluster 1 were significantly enriched in Alzheimer's disease and Huntington's disease pathways (Fig. S4). The top nine pathways we explored can influence the formation process of PAAD, and the FDP q-value and FWER *P*-value were <0.05. These results suggested a significant association between m^{6}A-related prognostic lncRNAs and the development of PAAD. By using GSEA, we were able to identify specific gene sets that were significantly enriched in each cluster, providing insights into the potential mechanisms underlying differential expression of m^{6}A-related prognostic lncRNAs in PAAD.

Our study revealed that the expression of m^{6}A-related prognostic lncRNAs in PAAD is associated with the immune response. Therefore, we further analyzed the infiltration characteristics of tumor microenvironment cells under different m^{6}A-related lncRNA patterns. To analyze tumor microenvironment infiltration in two different clustering patterns, 22 different immune cell types in 177 samples were evaluated by the CIBERSORT algorithm. We calculated the median absolute score for each cluster of 22 cell types given by CIBERSORT (Fig. S5A). The results showed that the scores of the naïve B cells, plasma cells, activated memory CD4 T cells, regulatory T cells (Tregs), and CD8 T cells in cluster 2 were significantly higher than those in cluster 1 (Fig. S5B—F). However, memory B cells and M1 and M2 macrophages in cluster 1 were significantly higher than those in cluster 2 (Fig. S5G—I). Then, we used the ESTIMATE algorithm to score the immune cell infiltration of patients in cluster 1 and cluster 2. Results demonstrated that cluster 2 showed higher ESTIMATE scores ($P < 0.01$), immune scores ($P < 0.01$), and stroma scores ($P < 0.01$) (Fig. S5J). The tumor microenvironment in cluster 2 significantly increased the infiltration of immune cells, thus confirming the above findings.

A total of 177 patient samples were randomly assigned to a training dataset ($n = 89$) and a test dataset ($n = 88$). Multivariate Cox regression and LASSO regression analysis were used to analyze the eleven m^{6}A-associated lncRNAs and establish a risk model with four m^{6}A-related lncRNAs (Fig. S6A, B). The patient samples in the training dataset were further divided into high-risk and low-risk groups based on the median risk score. The risk score distribution between the low-risk and high-risk groups is shown in Figure S6C. The survival status and survival time of patients in the two different risk groups are shown in Figure S6D. Survival analysis showed that the low-risk group had longer overall survival than the high-risk group ($P < 0.001$) (Fig. S6E). Figure S6F revealed the relative expression criteria of the four m^{6}A-associated lncRNAs in each patient. In addition, in the training dataset, the area under the curve of 5-year overall survival was 0.777, demonstrating that lncRNA features had good accuracy in predicting the prognosis of PAAD patients (Fig. S6G).

To test the prognostic ability of this established model, we calculated a risk score for each patient in the test group using a uniform formula. Figure 1A—C showed the

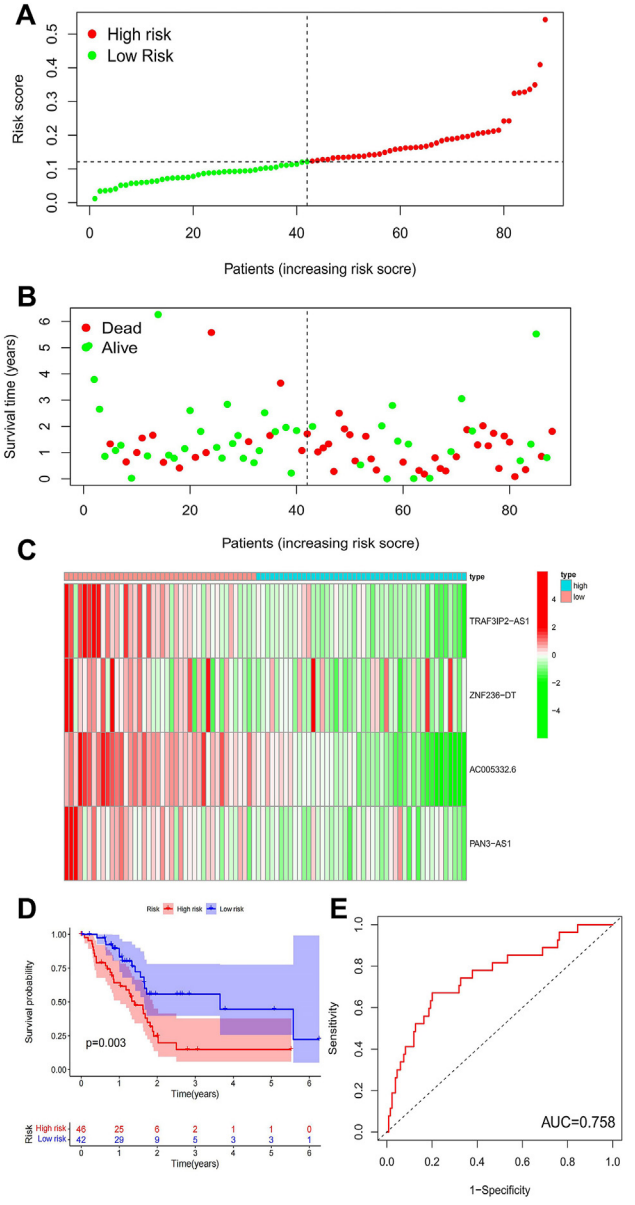

Figure 1 Verification of risk model. **(A)** The risk score distribution between the low-risk and high-risk groups of the test group. **(B)** The survival status and survival time of patients in the low-risk and high-risk groups of the test group. **(C)** Risk-related heatmap of four m^{6}A-related lncRNAs in the risk model of the test group. **(D)** The Kaplan—Meier survival curve of pancreatic adenocarcinoma samples in the test group. **(E)** ROC curve of the test group for evaluating the accuracy of the risk model.

distribution of risk scores in the test dataset, the pattern of survival status and time, and the expression of m^{6}A-related lncRNAs. The Kaplan—Meier survival analysis of the test groups showed no difference in outcomes in the training group (Fig. 1D, E).

Operating system differences were stratified according to prevailing clinicopathologic characteristics and analyzed between the low-risk and high-risk groups. Based on subgroups classified by sex, age, grade, or tumor stage, the low-risk group had better outcomes than the high-risk group, which suggested that our m^{6}A-related prognostic lncRNA risk model applied to different clinical subgroups (Fig. S7). Univariate and multivariate Cox analyses showed that m^{6}A-related lncRNA was the independent predictor of overall survival in PAAD, while they were uncorrelated with age, sex, grade, and stage (Fig. S8A, B).

Subgroup analysis of clustering showed that patients in cluster1 had a significantly higher risk score than patients in cluster2 ($P < 2.22e\text{-}16$) (Fig. S8C). Figure S8D showed that there were significant differences in clinical features between the high-risk group and the low-risk group. To explore the clinical significance of m^{6}A-related lncRNAs in PAAD, we compared the differences in risk scores between different PAAD subgroups. For the subgroup analysis of immune score, PAAD patients with high immuneScore had significantly lower risk scores than patients with low immuneScore ($P = 0.0021$) (Fig. S8E). Stratification of tumor size revealed that compared with T1—2 patients with PAAD, there was a remarkably higher risk score in T3—4 patients ($P = 0.0074$) (Fig. S8F). These results demonstrated that cluster, immune score, and primary tumor size were significantly associated with risk scores, while risk scores did not correlate with age, sex, grade, metastasis, lymph node, and stage (Fig. S8G). We found significant differences in PD-L1 expression between the low-risk and high-risk groups, revealing that the PAAD m^{6}A-related lncRNA risk model was closely related to PD-L1 expression (Fig. S9A).

Since the risk model showed a correlation with immune response, we further investigated the relationship between m^{6}A-related lncRNA risk model score and immune-infiltrating cells. Plasma cells, naïve B cells, activated memory CD4 T cells, CD8 T cells, and Tregs were negatively correlated with risk scores, while M0 macrophages, M2 macrophages, and activated natural killer cells were positively correlated with risk scores (Fig. S9B—I). All correlations were significant with $P < 0.05$. The baseline data of PAAD patients had no significant difference (Table S3). We performed additional experimental verification to calculate the relative expression levels of four types of prognostic-related lncRNAs in the tumor tissues of stage I and III patients by quantitative PCR (Fig. S9J). The results of experimental verification were basically consistent with the results of previous data analysis.

In conclusion, our study established a risk model based on four m^{6}A-related lncRNAs to predict tumor progression in patients with PAAD, which may become the potential prognostic factor. Besides, we found a significant correlation between m^{6}A-related prognostic lncRNAs and immune responses, which provides a novel insight into the exploration of biomarkers of immunotherapeutic responses in PAAD patients.

Ethics declaration

This study was approved by the Medical Research Ethics Committee of the First Affiliated Hospital of Nanchang University [reference number: (2023) CDYFYYLK (05—023)]. Participants involved in this study were provided with detailed information about the research objectives, procedures, potential risks, benefits, and their rights as participants.

Data availability

The microarray data were obtained from the GTEx, TCGA, TIMER, CCLE, GSEA and KEGG databases.

Conflict of interests

The authors declare that the research was conducted in the absence of any commercial or financial relationships that could be construed as a potential conflict of interests.

Appendix A. Supplementary data

Supplementary data to this article can be found online at https://doi.org/10.1016/j.gendis.2023.101141.

References

1. Rawla P, Sunkara T, Gaduputi V. Epidemiology of pancreatic cancer: global trends, etiology and risk factors. *World J Oncol*. 2019;10(1):10—27.
2. Baek B, Lee H. Prediction of survival and recurrence in patients with pancreatic cancer by integrating multi-omics data. *Sci Rep*. 2020;10(1):18951.
3. Wang T, Kong S, Tao M, Ju S. The potential role of RNA N6-methyladenosine in Cancer progression. *Mol Cancer*. 2020;19(1):88.
4. Chen L, Zhang J, Chen Q, et al. Long noncoding RNA SOX2OT promotes the proliferation of pancreatic cancer by binding to FUS. *Int J Cancer*. 2020;147(1):175—188.
5. Shi L, Hong X, Ba L, et al. Long non-coding RNA ZNFX1-AS1 promotes the tumor progression and metastasis of colorectal cancer by acting as a competing endogenous RNA of miR-144 to regulate EZH2 expression. *Cell Death Dis*. 2019;10:150.

Kaili Liao [a,1], Yuhan Xu [b,1], Bingying Lin [b,1], Yuxuan Xie [d,1], Qijun Yang [b], Wenyige Zhang [b], Beining Zhang [b], Jiarong Wen [e], Jingyi Wang [c], Zimeng Li [c], Yunqi Cheng [c], Xiaozhong Wang [a,*]

[a] *Jiangxi Province Key Laboratory of Laboratory Medicine, Jiangxi Provincial Clinical Research Center for Laboratory*

Medicine, Department of Clinical Laboratory, The Second Affiliated Hospital of Nanchang University, Nanchang, Jiangxi 330006, China
[b] *Queen Mary College of Nanchang University, Nanchang, Jiangxi 330001, China*
[c] *School of Public Health, Nanchang University, Nanchang, Jiangxi 330006, China*
[d] *The Second Clinical Medical College, Nanchang University, Nanchang, Jiangxi 330006, China*
[e] *The First Clinical Medical College of Nanchang University, Nanchang, Jiangxi 330006, China*

*Corresponding author.
E-mail address: xiaozhongwangncu@163.com (X. Wang)

18 May 2022
Available online 13 October 2023

[1] These authors contributed equally to this work.